4th URSI AT-RASC, Gran Canaria, 19-24 May 2024

Thermal Analysis of *Ex-Vivo* Liver RF Ablation through Numerical Modeling and Fiber Bragg Gratings Validation

Francesca Lodato*(1), Elena De Vita(2), Renato Patrone(3), Agostino Iadicicco(2), Stefania Campopiano(2), Francesco Izzo(3), Rita Massa(1), Daniele Riccio(4) and Giuseppe Ruello(4)

(1) Department of Physics "Ettore Pancini", University of Naples Federico II, Naples, Italy
(2) Department of Engineering, University of Naples "Parthenope", Naples, Italy
(3) Department of Abdominal Oncology – Division of Hepatobiliary Surgical Oncology, Istituto Nazionale Tumori - Fondazione G. Pascale – IRCCS, Naples, Italy
(4) Department of Electrical Engineering and Information Technology, University of Naples Federico II, Naples, Italy

Abstract

Radio frequency ablation is a well-established technique in clinical practice for the treatment of tumors. Standardized protocols, new electrode technologies, and impedance feedback generators have already made this technique very advantageous for both patient and doctors, providing minimal invasiveness and localized treatment. Treatment planning can further enhance this technique, creating a customized solution for each patient. Numerical methods are very helpful in predicting treatment outcomes. However, their use as a reference requires a high degree of accuracy. Aim of this paper is to combine the use of numerical simulations with experimental measurements based on fiber optic sensors. To do this, tests on ex-vivo porcine liver have been carried out using a bipolar probe. The results of simulations have been compared with punctual temperature data provided by optical fibers and with experimental outcomes showing a good agreement.

1. Introduction

In the last decades, radiofrequency ablation (RFA) has quickly developed into one of the most widespread alternative therapies to standard surgical resection, offering a minimally invasive and targeted approach for tumor treatment [1]. The RFA basic mechanism lies in the electrical alternating current flow through the tissues adjacent to the RF probe causing ionic agitation and thus frictional tissue heating. Such temperature increase results in coagulative necrosis of tissue, without removing it from the body, where the volume affected by the thermal damage is strictly related to the tissue temperature and the duration of heating [2].
In this framework, computational modeling plays a pivotal role in understanding the thermal dynamics that unfold during RFA and in predicting the treatment results in terms of extent of thermal injury within the treated tissue [3,4]. By providing insights into energy deposition, heat diffusion, and the overall thermal response, numerical simulations offer a powerful tool for treatment planning and optimization, allowing clinicians to tailor RFA parameters for different tumor types and sizes.
Parallelly, temperature monitoring becomes paramount for both numerical model validation and real time feedback for adapting the treatment settings to ensure an effective and safe ablation [5,6]. On this matter, fiber Bragg gratings (FBGs) represent an emerging technique for temperature measurements during thermal ablation thanks to their immunity to electromagnetic radiation, lightweight and small size, biocompatibility, multi-point sensing capability, and many other advantageous features [7,8].
Aim of this work is to compare numerical simulations with experimental temperature measurements based on FBG sensors during RFA of ex-vivo liver. In particular, a bipolar six-tips RF probe has been tested on liver samples, performing temperature monitoring by means of FBG sensors. The behavior of the probe has been numerically simulated by replicating the same configuration of the tips activation that happened during the experiments. This approach is very accurate to validate simulation results. Moreover, the simulation model herein implemented may be useful to design a specific treatment according to the single patient's characteristics. The work is divided into five sections. Following this introduction, in the second section the experimental set-up is described and a brief explanation of FBGs is reported. In the third section the implemented numerical simulations are introduced. Finally, the results and conclusion are presented.

2. Experimental Setup

For performing the experimental tests, the setup depicted in Figure 1 has been used. The employed bipolar probe (model SB Comb Array by LED SpA) is characterized by six tips which are autonomously activated in pairs by the system in an alternative manner based on the impedance values read by the RF generator (model Surtron SB by LED SpA). To carry out the thermal measurements during RFA, the probe was integrated with a FBG having a length of 5 mm and positioned in correspondence of the second and third electrode (see the zoom in Figure 1) for the first and the second test, respectively.

A FBG is an optical fiber portion affected by a spatially periodic perturbation of the refractive index of the core. Such a perturbation is responsible of the light reflection in a narrow range of wavelengths centered around a specific value λ_B (i.e., Bragg wavelength). The reflected spectrum shifts in response to external stimuli of strain and temperature variation, making the FBG sensitive to both these physical parameters.

For our purposes, to implement a strain-free sensing configuration and to protect the FBG during the tests, it was inserted into a needle made of carbon fiber (CF) with an outer radius of 0.35 mm and a thickness of 0.2 mm, glued to the electrode. Thus, the temperature variation ΔT experienced by the FBG can be obtained from:

$$\frac{\Delta\lambda_B}{\lambda_B} = S_T \Delta T \quad (1)$$

where $\Delta\lambda_B$ is the λ_B shift induced by ΔT, and S_T is the thermal sensitivity coefficient of the grating [9].

The $\Delta\lambda_B$ signals can be detected by the optical interrogation system (model FS-22 Bragg METER by HBM), which is able to detect them with a resolution of 1pm, enabling the temperature detection with a resolution of 0.1 °C with a minimum sampling frequency of 1 Hz. Then, the collected data can be displayed and post-processed by means of a PC.

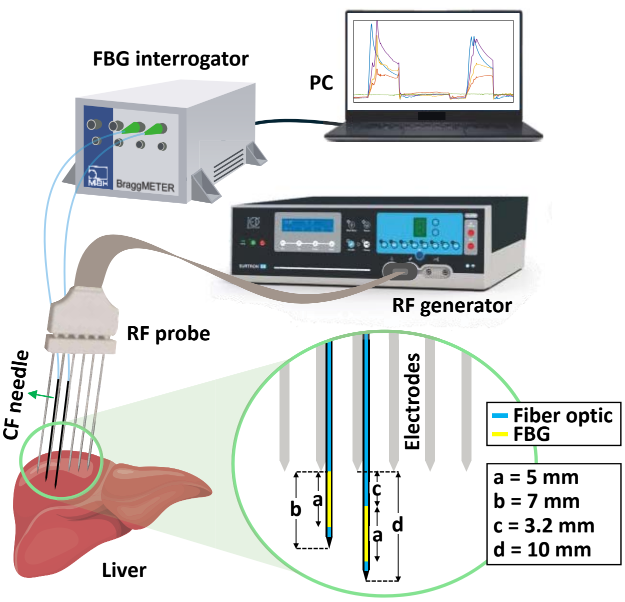

Figure 1. Experimental setup components with a zoom highlighting the arrangement of the FBG sensors.

3. Numerical Model

Numerical simulations have been performed using COMSOL Multiphysics. To reproduce RF ablation experiments, two physics have to be introduced in the model, whose detailed description can be found in [10,11]:

- AC/DC module for the electrical description;
- Heat transfer module for the thermal description;

The two physics are coupled to obtain the electric field distribution that generates the induced heating in the tissue. The model presented in this work consists of a liver of 10 cm x 10 cm x 10 cm in which the probe has been inserted at 3 cm depth. The geometry is reported in Figure 2.

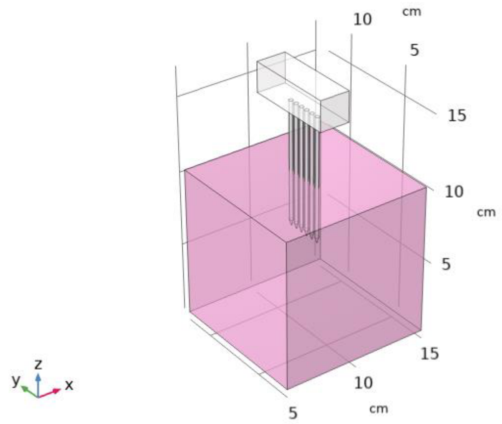

Figure 2. Model geometry in COMSOL Multiphysics.

Electrode tips have been characterized as Stainless Steel, a material already available in COMSOL library, while the liver tissue properties derive from different works present in literature [12,13]. In particular, the conductivity of the simulated liver is described with a liner variation with respect to the temperature as reported in [14]. To simulate the behavior of the RF generator, the tips have been activated alternatively from the outer to the inner ones in a bipolar configuration with a descending electric potential difference (i.e., 130 V, 90 V, 40 V). The order in which the electrodes have been switched on was different between the two experiments, according to the tissue impedance recorded by the generator. The analysis has been performed in different time intervals. In the first experiment, based on generator behavior, the intervals have been set as: 0 - 1 min; 1 min - 1.7 min; 1.7 - 2 min and finally 2 min up to 10 min. In the second experiment, the time intervals are: 0 - 1 min; 1 - 1.3 min; and 1.3 min up to 4 minutes. The results obtained in every time interval are used as initial conditions for the subsequent ones. The mesh size has been set as normal in every domain.

4. Results

The results of the simulations have been compared with experimental data collected in terms of ablation area and punctual temperature levels. In Figure 3 the comparison between simulated (on the left) and real (on the right) ablated zones are reported.

As it is possible to see, simulations and experimental results show good agreement. In particular, the ablated zone is comparable in terms of length and shape in the different shear axes.

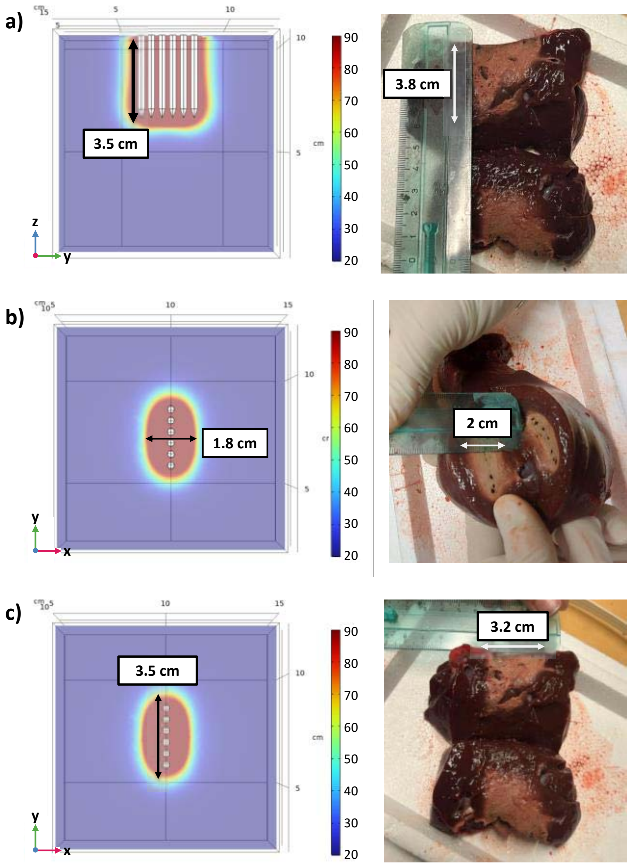

Figure 3. Comparison of ablation size obtained by simulations (left) and experiments (right) along z-axis (a), x-axis (b), and y-axis (c).

Moreover, a further validation has been made between the temperature profiles measured by means of the FBG and the ones estimated by the numerical model. In Figure 4 the comparison of temperature difference profiles with respect to initial temperature (20 °C) are reported.

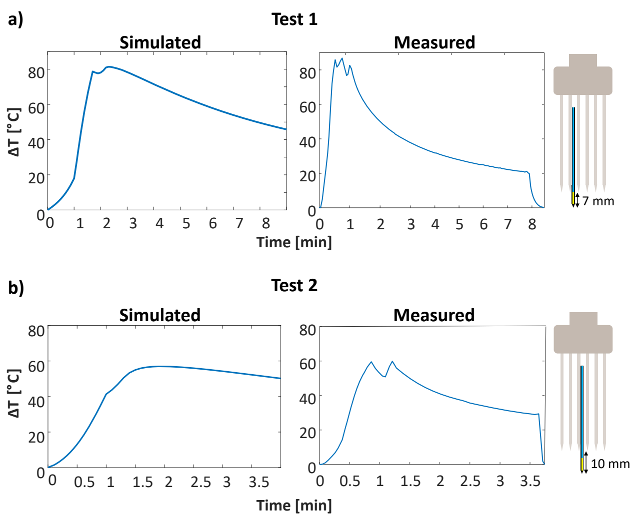

Figure 4. Comparison between simulated (left) and measured (right) temperature variation ΔT profile for the first (a) and second (b) experiment. The schematic beside the ΔT plots shows the position of the FBG sensor adopted in the respective test.

As shown in Figure 4, ΔT profiles are also in good agreement. In the first experiment, the maximum temperature difference value estimated by the simulations is 81 °C, while the value measured by the FBG is 86.9 °C. In the second experiment, the maximum ΔT value is 57 °C according to the simulations and 59.9 °C for the FBG sensor. Therefore, the model follows the trend of collected experimental data. The main differences between the temperature profiles are due to the randomly switch off and on of the source monitored by the FBG, and not considered in the simulation, and the slope of the descent curve. The latter discrepancy is motivated by the fact that the liver sample used for the experiments was 4-5 cm in size, while the simulated liver is bigger to avoid any boundary effects. So, the heat capacity of the simulated liver is bigger than the tested one.

5. Conclusions

Accurately predicting and estimating the ablated volume and the temperature within the target tissue during RFA improve the treatment outcomes both in terms of ablation safety (i.e., minimization of the collateral thermal damage to the nearby healthy anatomical structures) and efficient heating (i.e., complete tumor destruction to avoid recurrence). This is the reason why computational modeling of the phenomena occurring within the tissue undergoing RFA and real time temperature feedback provide a valuable tool to deeply understand, forecast, and control the therapy.
The present study focuses on both numerical simulation of RFA with a bipolar probe and FBG-based temperature measurements during RFA experimental tests on ex-vivo liver tissue, demonstrating that these tools can be combined in order to validate the numerical analysis through the recorded temperature data.
Results of simulation and experiments have been compared and show a good agreement in terms of length and shape of the ablated portion of tissue in the different shear axes and temperature profiles in correspondence of one of the RF probe electrodes.
In future developments more electrodes will be equipped with FBG sensors aiming to increase the number of sensing points within the ablation area. A greater number of measured points will be very useful for the comparison with simulation results to achieve higher accuracy levels. Moreover, further tests, considering also a bigger sample, will be helpful to check the numerical model in different experimental conditions.

References

[1] Ni, Y et al. "A review of the general aspects of radiofrequency ablation." *Abdominal imaging* vol. 30, 4, 2005, pp. 381-400. doi:10.1007/s00261-004-0253-9.

[2] K. Hong, C. Georgiades, “Radiofrequency ablation: mechanism of action and devices.” *Journal of vascular and interventional radiology : JVIR*, 21, 8, 2010, pp. S179-86, doi:10.1016/j.jvir.2010.04.008.

[3] G. Zorbas, T. Samaras, “Simulation of radiofrequency ablation in real human anatomy.” *International journal of hyperthermia: the official journal of European Society for Hyperthermic Oncology, North American Hyperthermia Group*, 30, 8, 2014, pp. 570-8, doi:10.3109/02656736.2014.968639.

[4] P. Voglreiter, P. Mariappan, M. Pollari, R. Flanagan, R. Blanco Sequeiros, R.H. Portugaller, J. Fütterer, D. Schmalstieg, M. Kolesnik, M. Moche, “RFA Guardian: Comprehensive Simulation of Radiofrequency Ablation Treatment of Liver Tumors”, *Sci Rep* 8, 787, 2018, doi: 10.1038/s41598-017-18899-2.

[5] G.C.M. van Erp, P. Hendriks, A. Broersen, C.A.M. Verhagen, F. Gholamiankhah, J. Dijkstra, M.C. Burgmans, “Computational Modeling of Thermal Ablation Zones in the Liver: A Systematic Review.” *Cancers*, 15, 23, 2023, pp. 5684, doi:10.3390/cancers15235684.

[6] C. Chang, H.-Y. Kuo, J.-P. Lee, “AC measurements and simulations of hepatic radiofrequency ablation.” *International journal of hyperthermia : the official journal of European Society for Hyperthermic Oncology, North American Hyperthermia Group*, 38, 1, 2021, pp. 1322-1332, doi:10.1080/02656736.2021.1971779.

[7] E. De Vita, D. Lo Presti, C. Massaroni, A. Iadicicco, E. Schena, S. Campopiano, “A review on radiofrequency, laser, and microwave ablations and their thermal monitoring through fiber Bragg gratings”, *IScience*, 26, 2023, pp. 108260, doi: 10.1016/j.isci.2023.108260.

[8] S. Mulier, Y. Jiang, J. Jamart, C. Wang, Y. Feng, G. Marchal, L. Michel, Y. Ni, “Bipolar radiofrequency ablation with 2 × 2 electrodes as a building block for matrix radiofrequency ablation: Ex vivo liver experiments and finite element method modelling.” *International journal of hyperthermia: the official journal of European Society for Hyperthermic Oncology, North American Hyperthermia Group*, 31, 6, 2015, pp. 649-65. doi:10.3109/02656736.2015.1046194.

[9] Q. Yu, Y. Zhang, Y. Dong, Y. P. Li, C. Wang and H. Chen, "Study on Optical Fiber Bragg Grating Temperature Sensors for Human Body Temperature Monitoring," *2012 Symposium on Photonics and Optoelectronics*, Shanghai, China, 2012, pp. 1-4, doi: 10.1109/SOPO.2012.6271111.

[10] M. Trujillo, E. Berjano, “Review of the mathematical functions used to model the temperature dependence of electrical and thermal conductivities of biological tissue in radiofrequency ablation.” *International journal of hyperthermia : the official journal of European Society for Hyperthermic Oncology, North American Hyperthermia Group*, 29, 6, 2013, pp. 590-7. doi:10.3109/02656736.2013.807438.

[11] I.A. Chang, U.D. Nguyen, “Thermal modeling of lesion growth with radiofrequency ablation devices.” *Biomedical engineering online*, 3, 1, 2004, art. no. 27, doi:10.1186/1475-925X-3-27.

[12] D. Deás Yero, F. Gilart González, D. Van Troyen and G. A. E. Vandenbosch, "Dielectric Properties of Ex Vivo Porcine Liver Tissue Characterized at Frequencies Between 5 and 500 kHz When Heated at Different Rates," in *IEEE Transactions on Biomedical Engineering*, 65, 11, 2018, pp. 2560-2568, doi: 10.1109/TBME.2018.2807981.

[13] S. Gabriel, R.W. Lau, C. Gabriel, “The dielectric properties of biological tissues: III. Parametric models for the dielectric spectrum of tissues”, *Phys. Med. Biol.*, 41, 1996, pp. 2271–2293, doi: 10.1088/0031-9155/41/11/003.

[14] S. Singh, R. Repaka, “Numerical investigation of convective cooling in minimizing skin burns during radiofrequency ablation of breast tumor”, *Sādhanā* 43, 6 2018, art. no. 90, doi: 10.1007/s12046-018-0872-4.